

Structural, morphological and optical properties of SnS₂ thin films by nebulized spray pyrolysis technique

K. Deva Arun Kumar¹ · S. Valanarasu¹ · V. Tamilnayagam^{2,3} · L. Amalraj³

Received: 9 February 2017 / Accepted: 2 June 2017 / Published online: 9 June 2017
© Springer Science+Business Media, LLC 2017

Abstract The thin films of Nano crystalline tin disulfide (SnS₂) have been prepared by nebulized spray pyrolysis technique (NSP) with different molar concentrations (0.3, 0.4 and 0.5 M). Cleaned glass substrates were used and the substrate temperature was maintained at 300 °C. The films were deposited using tin tetrachloride monohydrate (SnCl₄·H₂O) and thiourea in de-ionized water and Isopropyl alcohol (1:3 ratio). The prepared films structural, morphological and optical properties were studied using X-ray diffraction (XRD), scanning electron microscope (SEM), UV–Vis spectrophotometer. The structure of the films were found to be face centered cubic with preferential orientation along (002) plane. X-ray line profile analysis was used to evaluate the micro structural parameters such as crystallite size, micro strain, dislocation density and texture coefficient. The average crystallite size values are 60 nm. Morphological results of the SnS₂ thin films are small needle shaped particles and the average grain size was 400 nm. The optical studies revealed that the band gap between 2.65 and 2.72 eV and high optical transmittance 98%. EDAX spectrum of tin disulfide result showed some amount of

excess tin was present in the sample. This is the method with very low cost of producing tin disulfide (SnS₂) thin films, which is very important for many applications in industry.

1 Introduction

Physical properties and potential applications of semiconductor nanomaterials have been studied intensively [1, 2]. Nano materials have gained much attention among materials and their properties do not only depend on their composition but also on their shape and size distribution [3]. Among the different nanomaterials, perception the behavior of ferroelectric materials at the Nano scale is importance for the growth of molecular electronics [4]. In recent years, some researchers [5, 6] have been extensively investigated for their interesting physical and chemical properties with a potentially wide range of applications such as in improved catalysis, solar energy conversion, generation of hydrogen gas, and environmental purification. SnS₂ is a very important optical semiconductor, which can exhibit both P-type and N-type conduction, depending on the mole concentration of tin and sulfur [7]. The sulfide exists in variety of phase such as SnS, Sn₂S₃, Sn₃S₄ and SnS₂ due to bonding characteristics of tin and sulfur [8]. Among these semiconductors, tin disulfide (SnS₂) has attracted some attention due to its optical and structural properties [9]. Tin disulfide which is layered semiconductor belongs to a CdI₂-type structure with band gap of 2–3 eV [10, 11]. Broad band gap leads to photo conductance [12, 13] and makes it possible to be a candidate in solar cells and optoelectronic devices [14]. Other microelectronic packaging application, dielectric materials with a suitable dielectric constant, low

✉ V. Tamilnayagam
tamilnayagam.v@gmail.com

K. Deva Arun Kumar
apj.deva1990@gmail.com

L. Amalraj
amalraj57@yahoo.com

¹ PG and Research Department of Physics, Arul Anandar College, Karumathur, Madurai, India

² Department of Physics, A.P.A College of Arts and Culture, Palani, Tamilnadu, India

³ Research Department of Physics, V.H.N.S.N. College, Virudhunagar, Tamilnadu 626001, India

dielectric loss, high thermal conductivity and good thermal stability are required [15–17].

SnS_2 thin films have been deposited by variety of physical and chemical techniques, such as chemical vapour deposition (CVD) [18], chemical bath deposition, spray pyrolysis [19], electron beam induced deposition, molecular beam epitaxy [20] and vacuum evaporation [21], chemical deposition [22], dip coating [23]. All these reported methods require either relatively high reaction temperature or special reactors. Every technique of thin film deposition has its own advantages and disadvantages. But the Spray technique, which is economical, highly feasible for large area deposition and producing uniform, well adherent thin films is of interest to researchers. Compared to other methods, the nebulized spray pyrolysis (NSP) method is a simple, less expensive and less time consuming method.

In this paper, we are reporting the preparation and characterization of Nano crystalline SnS_2 thin films on glass substrates by (NSP) technique using $\text{SnCl}_4 \cdot \text{H}_2\text{O}$ and thiourea (ratio of 1:2) as the starting materials, with a different molar concentration and its structural, morphological and optical properties are studied using X-ray diffraction (XRD), scanning electron microscopy (SEM), EDAX analysis, FTIR and UV–Vis spectroscopy.

2 Experimental detail

2.1 Preparation of precursor solution

Nebulizer is an instrument for converting liquid into an aerosol. An aerosol is a suspension of small particles of liquid or solid in a gas. The tin disulfide films were deposited on glass substrate at a constant temperature of 300°C by nebulized spray pyrolysis technique at various molar

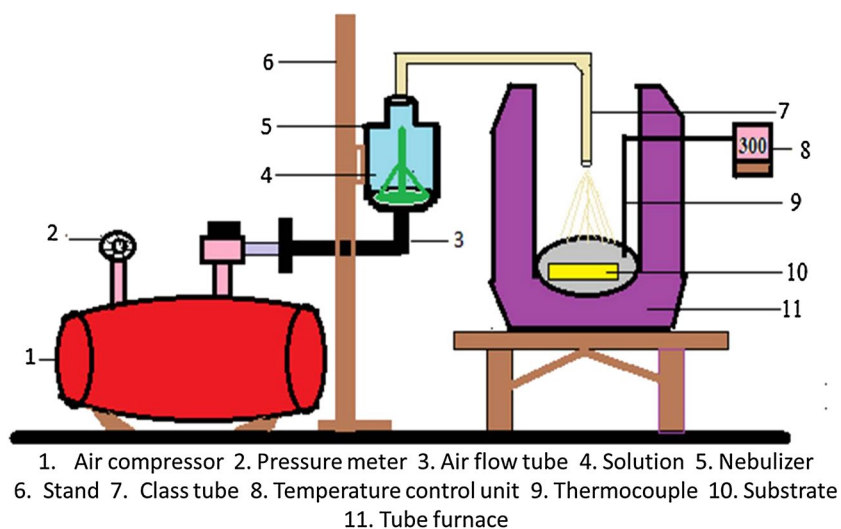
concentrations (0.3, 0.4 and 0.5 M). The nebulized spray pyrolysis method is very simple technique and low cost to produce SnS_2 thin films. In Fig. 1 the set up diagram of (NSP).

The starting solution was prepared using high purity $\text{SnCl}_4 \cdot \text{H}_2\text{O}$ and thiourea was dissolved separately in a solution containing de-ionized water and Isopropyl alcohol in the ratio of 1:3 by volume. The molarities of tin tetrachloride monohydrate and thiourea solutions were used 1:2 ratio respectively. A few drops of concentrated hydrochloric acid were added for complete dissolution. Equal volume of these two solutions were mixed and sprayed on to the glass substrate and carrier gas pressure was fixed at 0.7 kg/cm^2 . Distance between the glass tube and the substrate was maintained 2 cm. The total amount of spraying solution was 10 ml and the flow rate of the solution during spraying was adjusted to be 0.8 ml/m. After depositing the film it was allowed to cool to room temperature.

2.2 Characterization

X-ray diffraction (XRD) patterns of SnS_2 thin films were recorded by XPERT-PRO Diffractometer system using $\text{CuK}\alpha$ ($\lambda = 1.5406 \text{ nm}$) radiation with 2θ in the range 10° – 80° . The lateral morphology and roughness of the films were studied by means of scanning electron microscopy (SEM) using ZEISS system at the magnification of $\times 8000$. The EDAX spectrum of the thin films, binding energy region of 0.5–14 eV using BRUKER system. The optical absorption and transmittance study of SnS_2 films were performed in the wavelength range (350–1100 nm) using SHIMADZU 1800 (UV–Visible spectrophotometer). FTIR spectra for these samples were recorded using FTIR AFFINITY-1 spectrometer.

Fig. 1 Schematic diagram of the nebulizer spray pyrolysis (NSP) setup



3 Result and discussion

3.1 Structural studies

The X-ray diffraction (XRD) patterns of SnS₂ thin films prepared with different precursor molar concentration as shown in Fig. 2. The presence of single phase SnS₂ is seen from the Bragg peaks in the XRD pattern recorded over the thin films. From the XRD data, it is found that only one prominent peak (002) is clearly observed at all the three SnS₂ films, and also the (002) plane orientation become broad and strong crystalline. In general the broad peak is indicate that the film have nanocrystalline nature. Further, the broad peak is become slightly sharp position when increasing molar concentration. It reveals that the crystallinity of the films depends significantly on the molar concentration. The spectrum also contained another peak that correspond to (101) orientations, however this orientation has very poor intensity. The presence of all the two planes indicated that only SnS₂ phase had the hexagonal crystal structure. The structural data from the present studies were perfectly compared with JCPDS file number (89–3198).

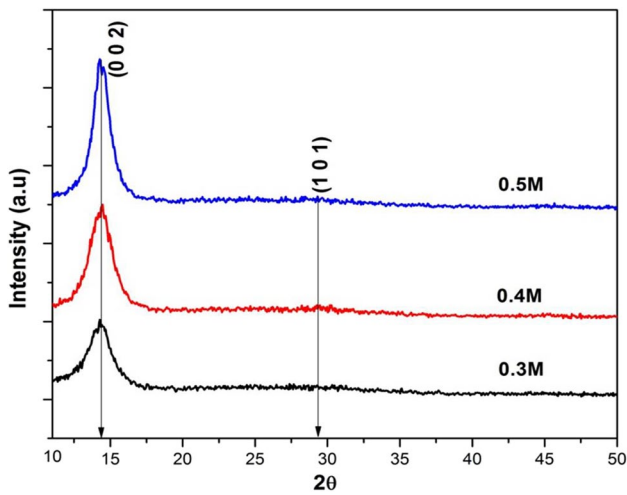


Fig. 2 XRD patterns of SnS₂ thin films of different molar concentrations

Table 1 Lattice parameters with d-spacing value compared to JCPDS file

Concentration (M)	2θ values	Miller indices (h k l)	d-spacing (Å)		JCPDS file no.: 89-3198		
			Observed value	JCPDS value	a=b=3.64	c=11.81	V=156.34
0.3	14.24	0 0 2	6.216	5.905	3.68	11.97	162.10
	28.8	1 0 1	3.082	3.051			
0.4	14.32	0 0 2	6.178	5.905	3.61	12.90	167.11
	28.6	1 0 1	3.119	3.051			
0.5	14.38	0 0 2	6.153	5.905	3.63	12.30	162.07
	29.0	1 0 1	3.041	3.051			

No other phases like SnS, Sn₂S₃, Sn₃S₄ were observed in the XRD spectrum, so our films have only single (SnS₂) phase. The presence of the SnS₂ peaks indicates that all the films were found to be nano sized crystalline nature. The peak intensity of the SnS₂ thin films gradually increases along with the increase in molar concentration. The crystallinity of the SnS₂ thin film is increases when increasing molar concentration is due to the reduction of full width at half maximum value and increase of peak intensity. A similar behavior was also observed by Abou-Helal et al. [24] in spray pyrolysis technique with respect to substrate temperature.

The lattice constants ‘a’ and ‘c’ for the hexagonal phase structure is determined by the relation,

$$\frac{1}{d^2} = \frac{4}{3} \left\{ \frac{h^2 + hk + k^2}{a^2} \right\} + \left\{ \frac{l^2}{c^2} \right\} \quad (1)$$

The lattice constants were calculated by taking an average of all the observed X-ray diffraction peaks. The average lattice constant was found to be a=3.68 and c=11.97, and the volume of unit cell V=162.10 which is slightly higher than the standard value (JCPDS file: V=156.34) of the hexagonal structure. This may be caused by the defect in the cell of the crystal, which causes local changes in the lattice parameters. The lattice parameters value and d-spacing values are compared with standard JCPDS results are shown in Table 1. From the full width at half maximum (FWHM) value of the peak obtained, the size of the crystallites formed in the SnS₂ thin film is determined using Debye–Scherrer formula [25, 26].

$$D = \frac{0.9\lambda}{\beta \cos \theta} \quad (2)$$

where k=0.9 is the shape factor, β is full-width at half maximum (FWHM) values, θ is the Bragg’s angle, λ is the X-ray wavelength (1.5406 Å).

The crystallite size was found to be (002) plane. The increasing molar concentration enhances the preferred orientation with the crystallite size increased due to the increasing (002) peak intensity. The increased molar concentration

may cause decrease of the density of nucleation centre's, and under these circumstances, a smaller number of centre's start to grow, which results in large crystallites [27]. Figure 3 shows the variation of FWHM and crystallite size along the (002) plane with different molar concentrations.

The micro strain and dislocation density of different molar concentration of SnS₂ thin films were calculated using the following equations [28, 29].

$$\varepsilon = \frac{\beta \cos \theta}{4} \quad (3)$$

$$\delta = \frac{1}{D^2} \quad (4)$$

The SnS₂ thin films with lower micro strain and dislocation density improve the crystallinity of the films which in turn increase the volumetric expansion of the films. Such a decrease in micro strain and dislocation density may be due to the decrease in lattice defects among the grain boundaries with the crystallite size increasing. Also the reduction of both (ε) and (δ) with molarity indicates the formation of high quality films at higher molar concentration.

A texture coefficient $TC(hkl)$ is calculated using the Harris analysis equation,

$$TC(hkl) = \frac{I(hkl)/I_0(hkl)}{N_r^{-1} \sum I(hkl)/I_0(hkl)} \quad (5)$$

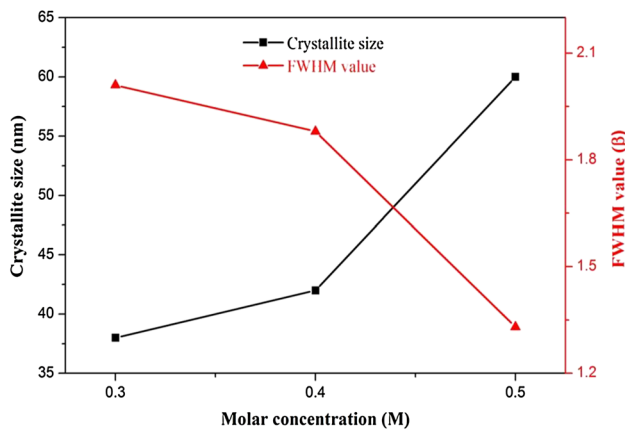


Fig. 3 Variation of crystallite size with FWHM values with different molar concentrations

Table 2 Structural parameters of SnS₂ thin films

Concentration (M)	Thickness (nm)	Crystallite size (nm)	Strain ($\times 10^{-3}$ lines ⁻² m ⁻⁴)	Dislocation density ($\times 10^{15}$ nm ⁻²)	$TC(002)$	Number of crystallite ($\times 10^{15}$)
0.3	381	38	8.695	0.685	1.42	6.84
0.4	471	42	8.132	0.551	1.55	6.09
0.5	593	60	5.750	0.275	1.65	2.71

where TC is the texture coefficients of the (hkl) plane, $I(hkl)$ the measured intensity, $I_0(hkl)$ the ASTM standard intensity of the corresponding powder, and N is the reflection number of significant peaks.

The texture coefficient is one of the basic structure parameters in all polycrystalline materials. For a film to have a preferential orientation at any (hkl) plane, the texture coefficient must be at least one. The value, $TC(hkl) = 1$, represents the thin film with randomly oriented crystallites, while higher value indicates the abundance of crystallites oriented along (hkl) direction. The value, $TC(hkl) > 1$, represents determined the preferential orientation and are related to the abundance of grains in a given (hkl) direction. The value, $TC(hkl) < 1$, represents indicates the lack of grains oriented in that direction. The TC values are slightly increased with increasing molar concentration is due to increasing crystallinity of the film.

The number of crystallites (N) per unit volume is calculated using the following formula,

$$N = \frac{t}{D^3} \quad (6)$$

where t is thickness and D is crystallite size of the SnS₂ thin films. The number of crystallites per unit area will be slightly decreased along with increasing thickness and crystallite size. The calculated values of micro structural parameters such as crystallite size (D), thickness (t), dislocation density (δ), micro strain (ε), texture coefficient 'TC' and the number of crystallites per unit area 'N' of (002) plane of the SnS₂ thin films are presented in Table 2.

3.2 Surface morphological studies

The Surface morphology of SnS₂ thin films were analyzed using scanning electron microscopy. SEM picture of SnS₂ thin films prepared at different molar concentrations (0.3–0.5 M) are shown in Fig. 4a–c. SEM results indicate that the average grain size and in which shape of the particles are presented for SnS₂ samples. The films have a compact and dense homogenous surface characterized by small grains observed in all the three samples. The SnS₂ thin films showed very small needle shaped particles and the surface discontinuities with an average grain size of 100–400 nm at different molar concentrations (0.3–0.5 M)

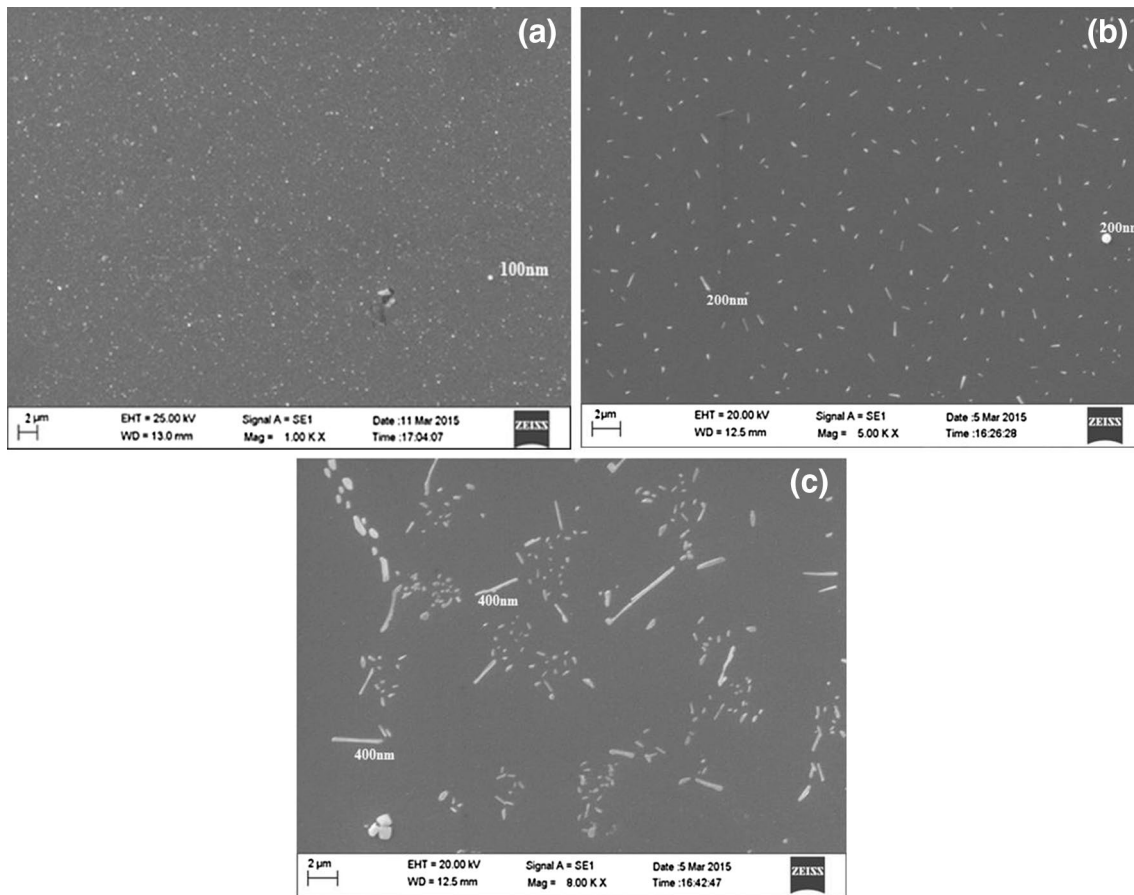


Fig. 4 SEM image of SnS_2 thin films at **a** 0.3 M, **b** 0.4 M and **c** 0.5 M concentrations

respectively. The grain size was found to be continuously increased with the increase of film thickness. The agglomeration seems isotropic for a particular needle shaped particle. Different needle shapes forms in different directions also shows various groups of grains are formed due to the SnS_2 samples. The lack of grain growth is possibly due to the limited surface diffusion length of the Sn and S adatoms. The observed grain size values from SEM images are much larger than the crystallite sizes measured from XRD peaks. This is due to the fact that in SEM images, the grain size is measured by the distance between the visible grain boundaries. Each grain constitutes aggregates of several crystallites [30].

3.3 Compositional study

Quantitative analysis of the film was carried out by using the EDAX technique to study stoichiometry of the film. The EDAX spectrum of the SnS_2 thin film at 0.3 M was recorded in the binding energy region of 0.5–14 eV as shown in Fig. 5. It is found that tin and sulfur are present in SnS_2 thin film and observed Tin(Sn) with 40%

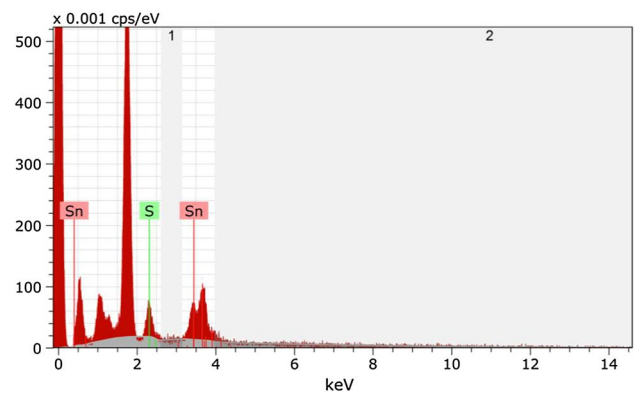


Fig. 5 EDAX spectrum of SnS_2 thin film at 0.3 M

and Sulfure(S) with 60% respectively, these report was in good agreement with Amalraj et al. [31]. Some amount of unreacted or (excess of) tin is present in the SnS_2 sample. Besides the Sn and S peaks, lines for Oxygen, Ca that could come from the glass substrate (not labeled here) is seen. Moreover, the ‘Si’ high intension peaks indicate the presence of this element either in the substrate or in the film.

EDAX analysis showed that the film deposited had almost a stoichiometric composition.

3.4 Optical studies

To study the optical properties of the materials, the optical absorption spectra of the film is recorded in wavelength range 350–1100 nm are shown in Fig. 6. Hence the optical transmittance (T) with respect to wavelength (λ) of nebulized spray pyrolysed SnS₂ thin film at different molar concentration is calculated and plotted as shown in Fig. 7. The optical transmittance spectra indicate a smooth increase and almost saturate at 98% in the visible region. Thin films optical transmittances 65–85% in the 500–800 nm wavelength ranges which is high enough for solar cell applications. Small maxima and minima in the transmittance curves appear due to the multiple interference effect. The multiple interference effect takes place due to high quality films and good surface properties [32]. The optical absorption slightly increases and transmittance slightly decreased along with increasing molar concentration 0.3, 0.4 and 0.5 M respectively. Thickness of the film ‘ t ’ is calculated using the wavelengths corresponding to the two successive transmittance maxima (λ_1, λ_2) or the minima (λ'_1, λ'_2) observed in the transmittance spectrum, in the formula [33].

$$\text{Maxima } t = \frac{\lambda_1 \lambda_2}{[2n(\lambda_2 - \lambda_1)]} \text{ (and) Minima } t = \frac{\lambda'_1 \lambda'_2}{[2n(\lambda'_2 - \lambda'_1)]} \tag{7}$$

where n is the refractive index and is the wavelength of transmittance spectra. The values of the thickness range from 371 to 93 nm for the different molarities (0.3–0.5 M) respectively.

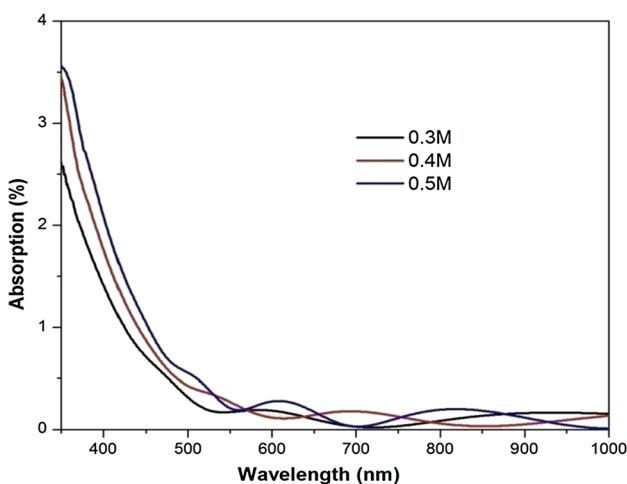


Fig. 6 A plot of absorption with wavelength of SnS₂ films

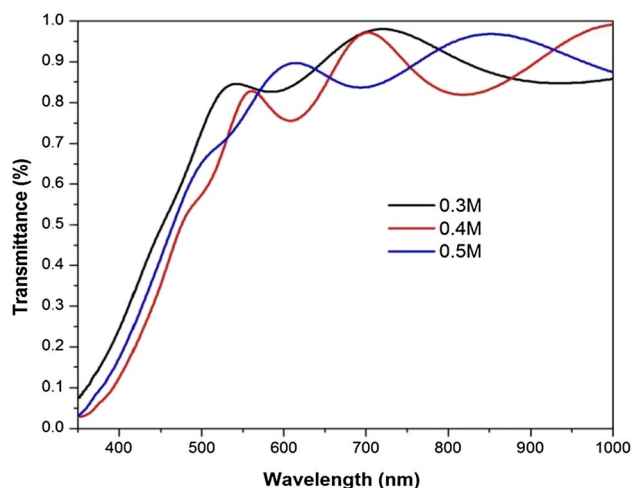


Fig. 7 Transmittance spectra of SnS₂ thin films

The direct allowed optical band gap of tin disulfide thin films has been determined from relation between the absorption coefficient (α) and the incident photon energy ($h\nu$) can be written as [34].

$$\alpha h\nu = B(h\nu - E_g)^n \tag{8}$$

where B and E_g are constant and optical band gap, respectively. The optical band gap of the SnS₂ thin films are shown in Fig. 8. The decrease in optical band gap with increasing molar concentrations can be due to the increase in the film thickness. The optical band gap values of SnS₂ thin film is decreased from 2.72 to 2.65 eV with increasing molar concentrations (0.3–0.5 M) respectively. This value is perfectly match with previous reported values [35, 36]. The variation of film thickness and band gap values with different molar concentrations are shown in Fig. 9. The small

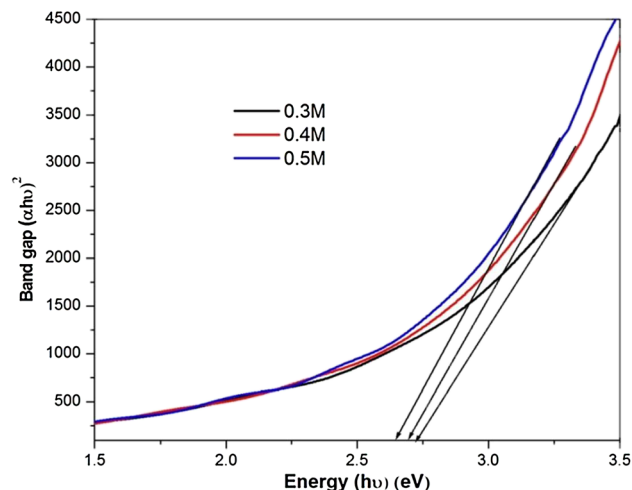


Fig. 8 Direct band gap ($\alpha h\nu$)² against energy (eV) for SnS₂ thin films

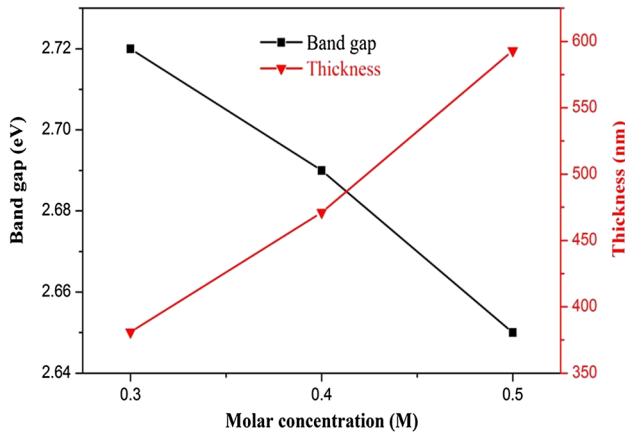


Fig. 9 The variation of film thickness and band gap values with different molar concentrations

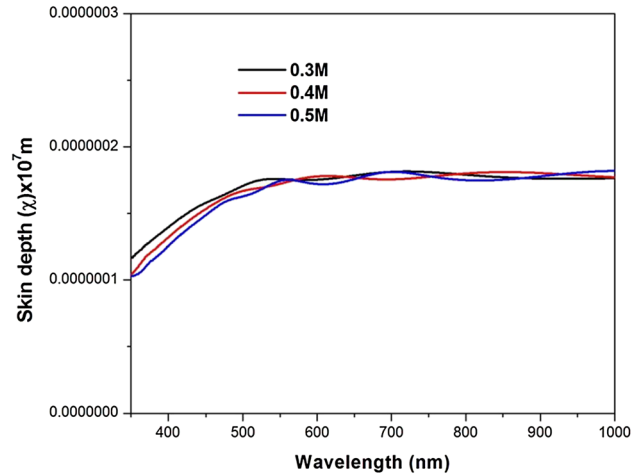


Fig. 11 Skin depth with different molar concentrations of SnS₂ thin films

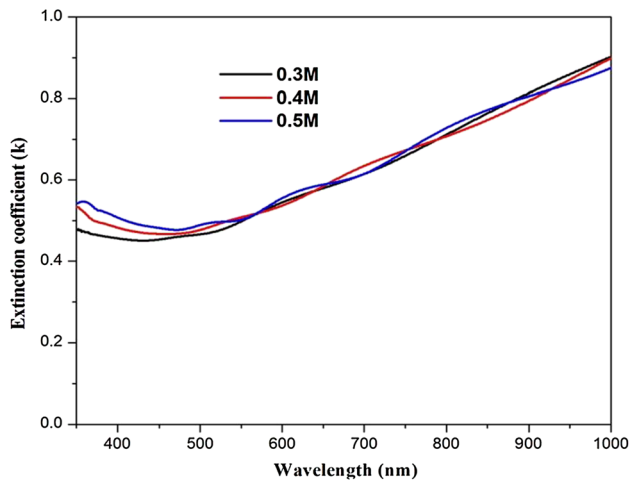


Fig. 10 Extinction coefficient with different molar concentrations of SnS₂ thin films

widening of the gap is due to the reduction of the disorder in the film [37].

The optical constants such as extinction coefficient (*k*) and skin depth (χ) can be obtained from the formula, were evaluated for SnS₂ films by using the relations,

$$k = \frac{\alpha \lambda}{4\pi} \tag{9}$$

$$\chi = \frac{\lambda}{2\pi k} \tag{10}$$

where α is the absorption coefficient, λ is the wavelength and *k* is the extinction coefficient values. Figures 10 and 11 shows the variation of both *k* and χ with wavelength for the layers grown with different molar concentration. The extinction coefficient value of the SnS₂ films is slightly

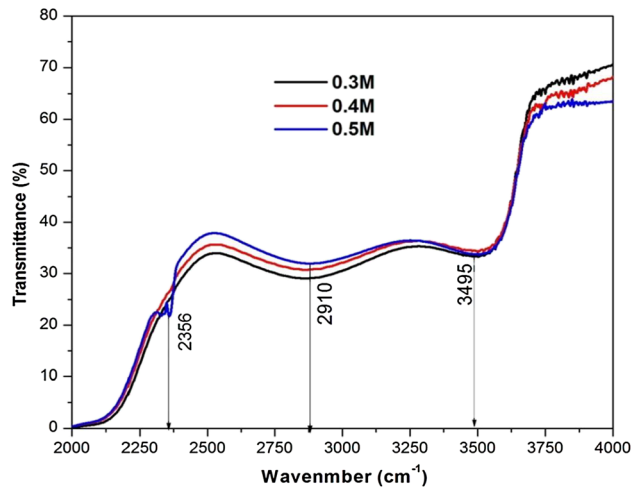


Fig. 12 FTIR spectra of SnS₂ thin films at different molar concentrations

increased in the range from 0.48 to 0.55 with increasing molarities. These values are good agreement with [38]. However, average skin depth of the films decreased (from 1.3 to 1.1 × 10⁷ m) with the increase of molarities.

3.5 FTIR studies

The Fourier transform infrared (FTIR) spectroscopy of the SnS₂ thin films at different molar concentrations were shown in Fig. 12. The presence of bonding between Sn and S atoms is estimated from the FTIR spectrum recorded using the as prepared samples. In the present study of the FTIR spectra of tin disulphide indicate a broad band at 3495 cm⁻¹ which corresponds to the vibration mode of O–H group indicating the presence of small amount

of water absorbed on the surface. The presence of strong C–H stretching at 2910 cm^{-1} is probably due to atmospheric moisture and CO_2 respectively, in the SnS_2 lattice. FTIR study of tin disulphide samples shows that the main band corresponding to the formation of vibration band at 2356 cm^{-1} attribute to the hydroxyl group, it is good agreement with Mariappan et al. [39]. Since SnS has no absorption peaks in the range of $2000\text{--}4000\text{ cm}^{-1}$.

4 Conclusion

Tin disulfide (SnS_2) thin films have been successfully deposited onto glass substrate from nebulized spray pyrolysis technique with different molar concentration. In our experiment, XRD studies show formation of pure SnS_2 films with hexagonal structures is identified. The optical band gap values both allowed and transition nature are good agreement with the reported value range of $2.65\text{--}2.72\text{ eV}$. The morphology of the deposited films has been found as smooth and needle shaped particle with coarser surface have discontinuities. The chemical constituents and their compositions of the films have been estimated by the energy dispersive X-ray analysis. From the various results for the properties of prepared nanocrystalline SnS_2 thin films conclude that it is a good candidate for solar cell and photo detector devices also can be tuned.

References

1. A. Sobhani-Nasab, Z. Zahraei, M. Akbari, M. Maddahfar, S.M. Hosseinpour-Mashkani, *J. Mol. Struct.* **1139**, 430–435 (2017)
2. S.M. Hosseinpour-Mashkani, A. Sobhani-Nasab, *J. Mater. Sci.* **28**, 43–45 (2017)
3. S.M. Hosseinpour-Mashkani, M. Maddahfar, A. Sobhani-Nasab, *S. Afr. J. Chem.* **70**, 44–48 (2017)
4. M. Salavati-Niasari, F. Soofivand, A. Sobhani-Nasab, M. Shakhouri-Arani, A.Y. Faal, S. Bagheri, *Adv. Powder Technol.* **27**, 2066 (2016)
5. A. Sobhani-Nasab, M. Behpour, *J. Mater. Sci.* **27**, 11946–11951 (2016)
6. A. Ziarati, A. Sobhani-Nasab, M. Rahimi-Nasrabadi, M.R. Ganjali, A. Badii, *J. Rare Earths* **35**(4), 374–381 (2017)
7. S.Y. Cheng, G.N. Chen, Y. Chen, et al, *Opt. Mater.* **29**, 439 (2006)
8. T. Jiang, G.A. Ozin, New directions in tin sulfide materials chemistry. *J. Mater. Chem.* **8**, 1099–1108 (1998)
9. C. Julien, M. Eddreif, I. Samaras, M. Balkanski, *Mater. Sci. Eng.* **B15**, 70 (1992)
10. Y.T. Qien, *Introduction to Crystal chemistry*, 2nd edn, vol 280. (Press of University of Science and Technology of China, Hefei, 1999)
11. G. Domingo, R.S. Itoga, C.R. Cannewurf, *Phys. Rev.* **143** 536 (1966)
12. S. Polarz, B. Smarsly, C. Goltner, M. Antonietti, *Adv. Matter.* **12**,1503 (2000)
13. M.J. Lanzafame, J. Michael, *Diss. Abstr. Int. B* **54**(1), 263 (1993)
14. J. Morales, V.C. Perez, J. Santos, L.J. Tirado, *J. Electrochem. Soc.* **143**(a), 2847 (1996)
15. G. Wu, Y. Cheng, K. Wang, Y. Wang, A. Feng, *J. Mater. Sci.* **27**, 5592–5599 (2016)
16. G. Wu, Y. Cheng, Y. Ren, Y. Wang, Z. Wang, H. Wu, *J. Alloys Compd.* **652**, 346–350 (2015)
17. G. Wu, J. Li, K. Wang, Y. Wang, C. Pan, A. Feng, *J. Mater. Sci. Mater. Electron* **28**, 6544–6551 (2017)
18. L.S. Price, I.P. Parkin, A.M.E. Handy, R.J.H. Clark, *Chem. Mater.* **11**, 1792–1799 (1999)
19. A. Ortiz, S. Lopez, *Semicond. Sci. Technol.* **9**, 2130 (1994)
20. K.W. Nnebesney, G.E. Collins, P.A. Lee, L.K. Chau, J. Danziger, E. Osburn, N.R. Armstrong, *Chem. Mater.* **3**, 829 (1991)
21. Joy George, K.S. Joseph, *J. Phys. D* **15**, 1109–1116 (1982)
22. C.D. Lokhande, *J. Phys. D* **23**, 1703 (1990)
23. S.K. Panda, A. Antonakos, *Mater. Res. Bull.* **42**, 576 (2007)
24. M.O. Abou-Helal, M. Boshta, *J. Am. Sci.* **8**, 61–63 (2012)
25. P.H. Klug, L.E. Alexander, *X-ray Diffractometers Producers.* (Wiley, New York, 1954)
26. B.D. Cullity, *Elements of X-ray Diffraction*, Biblio Bazaar, (2011)
27. J. Joseph, V. Mathew, K.E. Abraham, *Cryst. Res. Technol.* **41**, 1020 (2006)
28. R.R. Kasar, N.G. Despande, Y.G. Gudage, J.C. Vyas, R. Sharma, *Phys. B* **403**, 3724–3729 (2008)
29. R. Mariappan, M. Ragavendar, V. Ponnuswamy, *J. Alloys Compd.* **509**, 7337–7343 (2011)
30. R.N. Panda, M.F. Hsieh, R.J. Chung, T.S. Chain, *J. Phys. Chem. Solides* **64**, 193–199 (2003)
31. L. Amalraja, C. Sanjeevirajaa, M. Jayachandran, *J. Cryst. Growth* **234**(4), 683–689 (2002)
32. M. Abdel Rafea, N. Roushdy, *J. Phys. D* **42**, 015–413 (2009)
33. O.S. Heavens, *Optical Properties of Thin Solid Films.* (Dover Publications Inc., New York, 1965)
34. J. Tauc, *Amorphous and Liquid Semiconductors.* (Plenum Press, New York, 1974)
35. K. Vijayakumar, C. Sanjeeviraja, M. Jayachandran, L. Amalraj, *J. Mater. Sci.* **22**, 929–935 (2011)
36. I.B. Kherchachi, H. Saidi, A. Attaf, N. Attaf, A. Bouhdjar, *Optik* **127**, 4043–4046 (2016)
37. J.I. Pankove, *Optical Processes in Semiconductors.* (Dover, New York, 1975)
38. K.T.R. Reddy, G. Sreedevi, R.W. Miles, *J. Mater. Sci. Eng. A* **3**, 182–186 (2013)
39. R. Mariappan, M. Ragavendar, V. Ponnuswamy, *Opt. Appl.* **4**, 989–997 (2011)